Frustrated spin-$\frac{1}{2}$ J_1-J_2 Heisenberg ferromagnet on the square lattice studied via exact diagonalization and coupled-cluster method

J. Richter,[1] R. Darradi,[2] J. Schulenburg,[3] D. J. J. Farnell,[4] and H. Rosner[5]
[1]*Institut für Theoretische Physik, Universität Magdeburg, D-39016 Magdeburg, Germany*
[2]*Institut für Theoretische Physik, Technische Universität Braunschweig, D-38106 Braunschweig, Germany*
[3]*Universitätsrechenzentrum, Universität Magdeburg, D-39016 Magdeburg, Germany*
[4]*School of Community-Based Medicine, University of Manchester, Manchester, United Kingdom*
[5]*Max-Planck Institut für Chemische Physik fester Stoffe, D-01187 Dresden, Germany*
(Received 10 February 2010; revised manuscript received 30 April 2010; published 27 May 2010)

We investigate the ground-state magnetic order of the spin-$\frac{1}{2}$ J_1-J_2 Heisenberg model on the square lattice with ferromagnetic nearest-neighbor exchange $J_1<0$ and frustrating antiferromagnetic next-nearest-neighbor exchange $J_2>0$. We use the coupled-cluster method to high orders of approximation and Lanczos exact diagonalization of finite lattices of up to $N=40$ sites in order to calculate the ground-state energy, the spin-spin correlation functions, and the magnetic order parameter. We find that the transition point at which the ferromagnetic ground state disappears is given by $J_2^{c1}=0.393|J_1|$ (exact diagonalization) and $J_2^{c1}=0.394|J_1|$ (coupled-cluster method). We compare our results for ferromagnetic J_1 with established results for the spin-$\frac{1}{2}$ J_1-J_2 Heisenberg model with antiferromagnetic J_1. We find that both models (i.e., ferro- and antiferromagnetic J_1) behave similarly for large J_2, although significant differences between them are observed for $J_2/|J_1|\lesssim 0.6$. Although the semiclassical collinear magnetic long-range order breaks down at $J_2^{c2}\approx 0.6J_1$ for antiferromagnetic J_1, we do not find a similar breakdown of this kind of long-range order until $J_2\sim 0.4|J_1|$ for the model with ferromagnetic J_1. Unlike the case for antiferromagnetic J_1, if an intermediate disordered phase does occur between the phases exhibiting semiclassical collinear stripe order and ferromagnetic order for ferromagnetic J_1 then it is likely to be over a very small range below $J_2\sim 0.4|J_1|$.

DOI: 10.1103/PhysRevB.81.174429 PACS number(s): 75.10.Jm, 75.45.+j, 75.10.Kt

I. INTRODUCTION

The spin-$\frac{1}{2}$ Heisenberg antiferromagnet with nearest-neighbor (NN) J_1 and frustrating next-nearest-neighbor (NNN) J_2 coupling (J_1-J_2 model) on the square lattice has attracted much attention during the last twenty years (see, e.g., Refs. 1–21 and references therein). This model may serve as a canonical model to study the interplay of frustration effects and quantum fluctuations as well as quantum phase transitions driven by frustration.

The corresponding Hamiltonian reads

$$H = J_1 \sum_{\langle i,j\rangle} \mathbf{s}_i \cdot \mathbf{s}_j + J_2 \sum_{\langle\langle i,j\rangle\rangle} \mathbf{s}_i \cdot \mathbf{s}_j, \tag{1}$$

where the sums over $\langle i,j\rangle$ and $\langle\langle i,j\rangle\rangle$ run over all NN and NNN pairs, respectively, counting each bond once.

Recently, several quasi-two-dimensional magnetic materials with a ferromagnetic (FM) NN coupling $J_1<0$ and an antiferromagnetic (AFM) NNN coupling $J_2>0$ have been studied experimentally, e.g., $Pb_2VO(PO_4)_2$,[22–26] (CuCl)$LaNb_2O_7$,[27] $SrZnVO(PO_4)_2$,[25,28,29] $BaCdVO(PO_4)_2$,[24,28,30] and $PbZnVO(PO_4)_2$.[31] Due to a quite large AFM coupling J_2 these materials are driven out of the FM phase. These experimental studies have stimulated a series of theoretical investigations of the ground state (GS) and thermodynamic properties of the FM J_1-J_2 model, i.e., the model with FM NN exchange J_1 and frustrating AFM NNN exchange J_2.[32–40] It was found that the FM GS for the spin-$\frac{1}{2}$ model breaks down at $J_2=J_2^{c1}\approx 0.4|J_1|$.[32–34,37,40,41] Note that for the classical model ($s\to\infty$) the corresponding transition point is at $J_2=0.5|J_1|$. Moreover, for sufficiently large $J_2>J_2^{c2}$ a magnetically long-range ordered collinear stripe GS appears. According to Refs. 33, 34, 38, and 39, this second critical frustration strength is $J_2^{c2}\approx 0.6|J_1|$, and both magnetically ordered phases are separated by a magnetically disordered phase with enhanced nematic correlations. Note that this collinear stripe GS phase, as well as the values of J_2^{c1} and J_2^{c2} reported in the literature, are similar to the observation for the corresponding AFM model, i.e., the model with AFM J_1.[1,4,6–8,10,12–14,16–21]

As we know from the investigation of the AFM J_1-J_2 model the study of the GS phases in the strong frustration regime, i.e., $J_2\sim 0.5J_1$, is one of the hardest problems in the field of frustrated quantum magnetism. In the meantime, scores of papers have dealt with this problem. On the other hand, for the FM J_1-J_2 model so far only a few studies exist. Hence, further investigations using alternative approaches are highly desirable to confirm or to query the existing results.

Due to frustration, highly efficient quantum Monte Carlo codes, such as the stochastic series expansion suffer from the minus sign problem. Therefore, many other approximate methods, e.g., the Green's function method,[11,14,40] the series expansion,[12,13,18] the Schwinger boson approach,[8] variational techniques,[10] the functional renormalization group technique[21] as well as the projected entangled pair states method[19] were used to study the GS phases of the model with AFM J_1.

In the present paper, we calculate the GS energy, spin-spin correlation functions, and the magnetic order parameter of the collinear stripe order using two completely different methods, namely, a large-scale exact diagonalization (ED) of

TABLE I. Singlet GS energy per site E_0/N and square of order parameter $M_N^2(0,\pi)$, cf. Eq. (2), for the J_1-J_2 model with $J_1=-1$ on finite square lattices of $N=32$, 36, and 40 sites.

	$N=32$	$N=32$	$N=36$	$N=36$	$N=40$	$N=40$
J_2	E_0/N	$M_N^2(0,\pi)$	E_0/N	$M_N^2(0,\pi)$	E_0/N	$M_N^2(0,\pi)$
0.40	−0.31284253	0.11167341	−0.31431081	0.08925821	−0.31127637	0.10687524
0.45	−0.34234578	0.12363200	−0.34259033	0.11439947	−0.34062128	0.11332095
0.50	−0.37406800	0.12617129	−0.37369533	0.11854042	−0.37174835	0.11581048
0.55	−0.40673497	0.12730259	−0.40577614	0.12049011	−0.40374930	0.11719238
0.60	−0.43994975	0.12793318	−0.43841728	0.12170653	−0.43628038	0.11810286
0.65	−0.47352394	0.12833506	−0.47143169	0.12256200	−0.46917022	0.11876286
0.70	−0.50735237	0.12861459	−0.50471467	0.12320526	−0.50231993	0.11927048
0.80	−0.57553353	0.12898259	−0.57184472	0.12411474	−0.56916790	0.12000667
0.90	−0.64418634	0.12921694	−0.63949153	0.12472863	−0.63652042	0.12051714
1.00	−0.71315309	0.12937976	−0.70748822	0.12516916	−0.70421577	0.12089143

finite lattices up to $N=40$ sites (see Sec. II) and the coupled-cluster method (CCM) (see Sec. III). Both methods have been successfully applied to the AFM J_1-J_2 model, see e.g., Refs. 2–6 and 20 for the ED method and Refs. 9 and 14–17 for the CCM. Henceforth, we set $|J_1|=1$ if not stated otherwise explicitly.

II. RESULTS OF LANCZOS EXACT DIAGONALIZATION FOR FINITE SQUARE LATTICES

The paper of Schulz and co-workers,[4] presenting results for finite lattices up to $N=36$ sites for the first time has set a benchmark for ED studies of quantum Heisenberg magnets. Frequently, such numerical exact results are also used to test new approximate methods, see, e.g., Refs. 17, 42, and 43. Due to the progress in the computer hardware and the increased efficiency in programming, very recently the GS and low-lying excitations of the unfrustrated (i.e., $J_2=0$)[44] as well as the frustrated spin-$\frac{1}{2}$ HAFM[20] and of a spin-$\frac{1}{2}$ Heisenberg model with ring exchange[45] have been calculated by the Lanczos algorithm for a square lattice with $N=40$ sites. The largest two-dimensional quantum spin model for which the GS has been calculated so far is the spin-$\frac{1}{2}$ HAFM on the star lattice with $N=42$ sites.[46] Note, however, that for sectors of $S_z>0$ which are relevant for finite magnetic fields much larger system sizes can be treated by ED, see, e.g., Ref. 47.

In order to analyze GS magnetic ordering, the spin-spin correlation functions and an appropriate order parameter are important quantities. Following Schulz *et al.*,[4] we use here the **Q**-dependent susceptibility (square of order parameter) defined as

$$M_N^2(\mathbf{Q}) = \frac{1}{N(N+2)} \sum_{i,j} \langle \mathbf{s}_i \cdot \mathbf{s}_j \rangle e^{i\mathbf{Q}(\mathbf{R}_i - \mathbf{R}_j)}. \tag{2}$$

The relevant order parameter for the collinear stripe magnetic long-range order (LRO) present at large J_2 is $M_N^2(\mathbf{Q})$ at the magnetic wave vectors $\mathbf{Q}_1=(\pi,0)$ or $\mathbf{Q}_2=(0,\pi)$. In Table I, we give the singlet GS energies per site as well as the order parameters $M_N^2(0,\pi)$ for finite lattices of $N=32$, 36, and 40 sites. In a second Table II, we present the spin-spin correlation functions $\langle \mathbf{s}_0 \cdot \mathbf{s}_\mathbf{R} \rangle$ for the largest lattice considered. There are in total 11 different correlation functions for $N=40$ that are given in Table II for the same data points as in Table I. Periodic boundary conditions are imposed for all of the lattices employed here. A graphical representation of the finite lattices can be found in Refs. 4 and 20. The exact data, which is provided here in some detail in the tables, might be used as benchmark data for approximate methods applied to this model.[48]

The corresponding data for the energies, the square of order parameters and for some selected correlation functions are also displayed in more detail in Figs. 1–3. By way of comparison, we also present corresponding curves for the AFM model ($J_1=+1$).[20] We recall that the GS is identical for the FM and the AFM model on the classical level for $J_2>0.5$. For the spin-$\frac{1}{2}$ model, due to quantum fluctuations, the two models behave differently. Only in the limit $J_2\to\infty$ the sign of J_1 becomes irrelevant for the quantum GS. Our numerical data for the GS energy, the order parameter, and the spin-spin correlation functions demonstrate that for $J_2 \gtrsim 0.8$ the different models behave qualitatively very similarly. Note, however, that due the different sign in the NN exchange J_1, also the NN spin-spin correlation $\langle \mathbf{s}_0 \cdot \mathbf{s}_\mathbf{R} \rangle$, $\mathbf{R}=(1,0)$, has a different sign for the models. In the region $0.8 \gtrsim J_2 \gtrsim 0.6$ the differences between both models become more and more pronounced. For $J_2 \lesssim 0.6$ both models behave completely differently. From many previous studies[1–20] we know that $J_2 \approx 0.6$ is the point where for the AFM model the semiclassical collinear stripe LRO gives way for a magnetically disordered phase. It is obvious that at $J_2 \approx 0.6$ the order parameter $M_N^2(0,\pi)$ of the AFM model changes drastically (cf. Figure 2), whereas $M_N^2(0,\pi)$ remains almost constant up to about $J_2 \approx 0.45$ for the FM model, i.e., there is no indication for a breakdown of semiclassical magnetic LRO around $J_2 \approx 0.6$ for $J_1=-1$. Only for $J_2 \lesssim 0.45$ there is a noticeable decrease in the order parameter $M_N^2(0,\pi)$ until the transition point J_2^{c1} between the singlet GS and the fully polarized FM GS. Note, however, that $M_N^2(0,\pi)$ remains finite until J_2^{c1}. The different behavior of both models can also be seen in the

TABLE II. Spin-spin correlation functions $\langle \mathbf{s}_0 \cdot \mathbf{s}_\mathbf{R} \rangle$ for the J_1-J_2 model with $J_1=-1$ on the finite square lattice of $N=40$ sites.

J_2	$\langle \mathbf{s}_0 \cdot \mathbf{s}_\mathbf{R} \rangle$ $\mathbf{R}=(1,0)$	$\langle \mathbf{s}_0 \cdot \mathbf{s}_\mathbf{R} \rangle$ $\mathbf{R}=(2,0)$	$\langle \mathbf{s}_0 \cdot \mathbf{s}_\mathbf{R} \rangle$ $\mathbf{R}=(3,0)$	$\langle \mathbf{s}_0 \cdot \mathbf{s}_\mathbf{R} \rangle$ $\mathbf{R}=(3,1)$	$\langle \mathbf{s}_0 \cdot \mathbf{s}_\mathbf{R} \rangle$ $\mathbf{R}=(2,1)$	$\langle \mathbf{s}_0 \cdot \mathbf{s}_\mathbf{R} \rangle$ $\mathbf{R}=(1,1)$
0.40	0.044832	0.183933	0.012219	−0.194442	−0.040218	−0.277017
0.45	0.033144	0.196362	0.014787	−0.199197	−0.033852	−0.304812
0.50	0.027648	0.201318	0.014973	−0.200208	−0.029595	−0.316452
0.55	0.024204	0.204078	0.014523	−0.200667	−0.026460	−0.323037
0.60	0.021753	0.205887	0.013884	−0.201012	−0.024012	−0.327312
0.65	0.019875	0.207189	0.013203	−0.201327	−0.022023	−0.330324
0.70	0.018363	0.208185	0.012537	−0.201621	−0.020367	−0.332568
0.80	0.016044	0.209616	0.011328	−0.202149	−0.017745	−0.335676
0.90	0.014313	0.210600	0.010293	−0.202593	−0.015750	−0.337719
1.00	0.012954	0.211320	0.009417	−0.202962	−0.014172	−0.339156

J_2	$\langle \mathbf{s}_0 \cdot \mathbf{s}_\mathbf{R} \rangle$ $\mathbf{R}=(1,2)$	$\langle \mathbf{s}_0 \cdot \mathbf{s}_\mathbf{R} \rangle$ $\mathbf{R}=(1,3)$	$\langle \mathbf{s}_0 \cdot \mathbf{s}_\mathbf{R} \rangle$ $\mathbf{R}=(2,2)$	$\langle \mathbf{s}_0 \cdot \mathbf{s}_\mathbf{R} \rangle$ $\mathbf{R}=(2,3)$	$\langle \mathbf{s}_0 \cdot \mathbf{s}_\mathbf{R} \rangle$ $\mathbf{R}=(4,-2)$
0.40	−0.027909	−0.177408	0.160527	−0.007815	0.154329
0.45	−0.023862	−0.183867	0.176142	−0.003522	0.166329
0.50	−0.021057	−0.186297	0.181923	−0.002268	0.169644
0.55	−0.018936	−0.187719	0.185043	−0.001671	0.171225
0.60	−0.017247	−0.188748	0.187071	−0.001323	0.172227
0.65	−0.015858	−0.189567	0.188526	−0.001098	0.172968
0.70	−0.014691	−0.190248	0.189642	−0.000936	0.173562
0.80	−0.012825	−0.191325	0.191262	−0.000723	0.174483
0.90	−0.011394	−0.192135	0.192387	−0.000588	0.175173
1.00	−0.010260	−0.192765	0.193215	−0.000498	0.175707

GS energy and the spin-spin correlation functions, cf. Figures 1 and 3. From Fig. 1 it is evident that the finite size-effects in the GS energy E_0 of the FM model are small. In fact, the difference in E_0 between $N=36$ and $N=40$ is less than 1% in the whole region shown in Fig. 1. Hence, a finite-size extrapolation should give accurate results for the GS energy (see below).

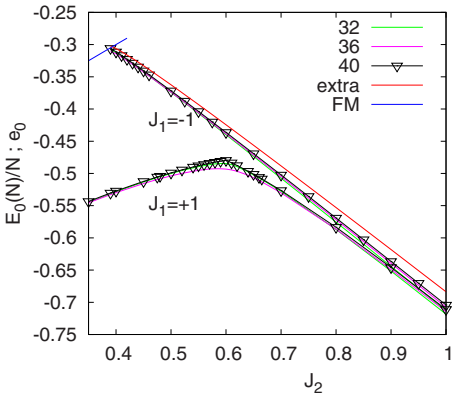

FIG. 1. (Color online) GS energy per site $E_0(N)/N$ calculated by ED for finite lattices of $N=32,36,40$ sites as well as the extrapolated value e_0 $(N\to\infty)$, cf. Equation (3). For comparison we show also $E_0(N)/N$ for the AFM model $(J_1=+1)$ with $N=32,36,40$ (Ref. 20). The blue line shows the energy of the FM eigenstate.

Following the lines of Refs. 4 and 20 we use now the data for $N=20,32,36,40$ to perform a finite-size extrapolation. Note that we do not include the data for the lattice with $N=16$ sites, since this lattice exhibits an anomalous behavior.[4] The finite-size extrapolation rules in a two-dimensional magnetically ordered phase are well known.[49,50] The finite-size behavior of the GS energy is given by

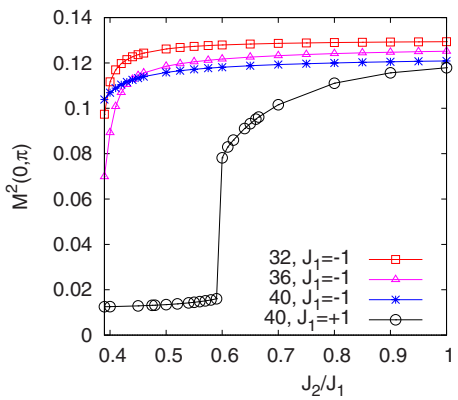

FIG. 2. (Color online) Square of order parameters $M_N^2(0,\pi)$, see Eq. (2), for $N=32$, 36, and 40 $(J_1=-1)$. For comparison we also present a corresponding curve for the AFM model $(J_1=+1)$ for $N=40$.

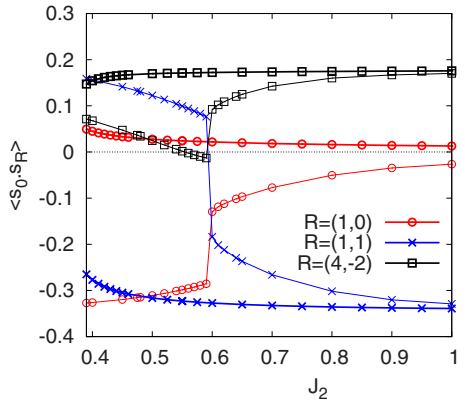

FIG. 3. (Color online) Selected spin-spin correlation functions $\langle \mathbf{s}_0 \cdot \mathbf{s}_\mathbf{R} \rangle$ calculated with Lanczos ED for $N=40$ (thick lines: $J_1=-1$, thin lines $J_1=+1$).

$$\frac{E_0(N)}{N} = e_0 - \frac{\text{const}}{N^{3/2}} + \cdots . \tag{3}$$

The extrapolated energy e_0 is shown in Fig. 1. We use the intersection point between the extrapolated singlet GS energy e_0 and the energy of the fully polarized FM GS to determine the transition point between both GS phases to $J_2^{c1}=0.393$.

The order parameter for the collinear stripe LRO in the thermodynamic limit is defined as[4,20] $m_s = \sqrt{8}\lim_{N\to\infty} M_N(0,\pi)$. The finite-size behavior of $M_N(0,\pi)$ is given by

$$M_N^2(\pi,0) = \frac{1}{8}m_s^2 + \frac{\text{const}}{\sqrt{N}} + \cdots . \tag{4}$$

However, from Fig. 2 it is evident that the finite-size behavior of $M_N^2(\pi,0)$ becomes irregular at $J_2=0.44$, since we have $M_{40}^2(\pi,0) > M_{36}^2(\pi,0)$ for $J_2^{c1} < J_2 < 0.44$. For illustration we show the extrapolation of the $M_N^2(\pi,0)$ data for $J_2=0.8$ and $J_2=0.44$ in the inset of Fig. 4. Hence, the extrapolation of $M_N^2(\pi,0)$ becomes inconclusive in that region. The results for m_s for $J_2 \geq 0.44$ are shown in Fig. 4. For comparison we show also the extrapolated order parameter for the AFM model.[20] Although m_s becomes zero at $J_2^{c2} \approx 0.66 J_1$ for the AFM model, we do not find an indication for a magnetically disordered phase in the region above $J_2=0.44$ for the FM model. However, we cannot exclude such a GS phase in the very small parameter region located between $J_2=0.393$ and $J_2=0.44$ from our ED data.

III. RESULTS OF THE CCM FOR THE INFINITE SQUARE LATTICE

For the sake of brevity, we will illustrate only some important aspects of the CCM. The interested reader can find more details concerning the application of the CCM on the AFM J_1-J_2 model in Refs. 9 and 15–17. For more general information on the methodology of the CCM, see, e.g., Refs. 51–53.

First we notice that the CCM approach automatically yields results in the thermodynamic limit $N\to\infty$. The starting

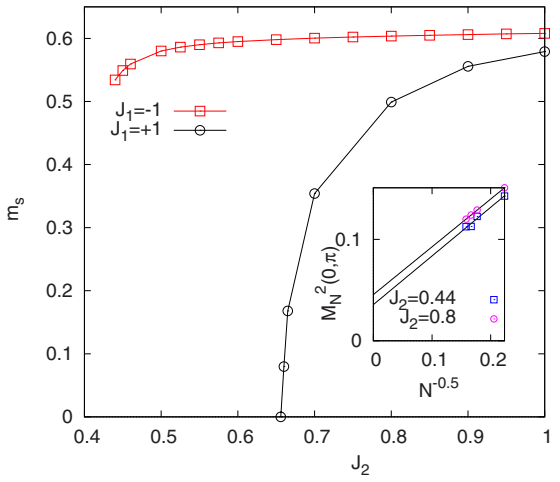

FIG. 4. (Color online) Extrapolated order parameters m_s, see Eq. (4), for the FM model ($J_1=-1$) and the AFM model ($J_1=+1$). Inset: Illustration of the finite-size extrapolation of the square of order parameter $M_N^2(0,\pi)$ according to Eq. (4) for $J_2=0.44$ and $J_2=0.8$.

point for a CCM calculation is the choice of a normalized reference (or model) state $|\Phi\rangle$. We then define a set of mutually commuting multispin creation operators C_I^+ with respect to this state, which are defined over a complete set of many-body configurations I. For the system under consideration here we choose one of the two degenerate classical collinear stripe states as the reference state. Next, we perform a rotation of the local axis of the spins such that all spins in the reference state align along the negative z axis. In the rotated coordinate frame the reference state reads $|\Phi\rangle = |\downarrow\rangle|\downarrow\rangle|\downarrow\rangle\ldots$, and we can treat each site equivalently. The corresponding multispin creation operators then can be written as $C_I^+ = s_i^+,\ s_i^+ s_j^+,\ s_i^+ s_j^+ s_k^+, \cdots$, where the indices $i,j,k,\ldots$ denote arbitrary lattice sites.

The CCM parametrizations of the ket- and bra-GS's are given by

$$H|\Psi\rangle = E|\Psi\rangle; \quad \langle\tilde{\Psi}|H = E\langle\tilde{\Psi}|;$$

$$|\Psi\rangle = e^S|\Phi\rangle, \quad S = \sum_{I\neq 0} \mathcal{S}_I C_I^+;$$

$$\langle\tilde{\Psi}| = \langle\Phi|\tilde{S}e^{-S}, \quad \tilde{S} = 1 + \sum_{I\neq 0} \tilde{\mathcal{S}}_I C_I^- . \tag{5}$$

We wish to determine the correlation coefficients $\mathcal{S}_I$ and $\tilde{\mathcal{S}}_I$ for the correlation operators S and $\tilde{S}$. By using the Schrödinger equation, $H|\Psi\rangle = E|\Psi\rangle$, we can write the GS energy as $E = \langle\Phi|e^{-S}He^S|\Phi\rangle$. The magnetic order parameter is given by

$$m_s = -\frac{1}{Ns}\sum_{i=1}^{N} \langle\tilde{\Psi}|s_i^z|\Psi\rangle, \tag{6}$$

where s_i^z is expressed in the rotated coordinate system and $s=1/2$ is the spin quantum number. To find the ket-state and bra-state correlation coefficients we have to solve the so-called CCM ket- and bra-state equations given by

$$\langle \Phi | C_I^- e^{-S} H e^S | \Phi \rangle = 0, \quad \forall\, I \neq 0, \tag{7}$$

$$\langle \Phi | \tilde{\mathcal{S}} e^{-S} [H, C_I^+] e^S | \Phi \rangle = 0, \quad \forall\, I \neq 0. \tag{8}$$

Each ket- or bra-state equation belongs to a certain creation operator $C_I^+ = s_i^+,\ s_i^+ s_j^+,\ s_i^+ s_j^+ s_k^+, \cdots$, i.e., it corresponds to a certain set (configuration) of lattice sites $i, j, k, \ldots$.

For the considered quantum many-body model we have to use approximations in order to truncate the expansion of S and $\tilde{S}$. We use the well established LSUBn scheme[15–17,51–55] in which all multispin correlations in the correlation operators S and $\tilde{S}$ over all distinct locales on the lattice defined by n or fewer contiguous sites are taken into account. For instance, within the LSUB4 approximation, multispin creation operators of one, two, three or four spins distributed on arbitrary clusters of four contiguous lattice sites are included. The number of these fundamental configurations can be reduced by using lattice symmetry and conservation laws. In the highest order of approximation considered here, namely, the LSUB10 approximation, we have finally 45825 fundamental configurations for the collinear stripe reference state, yielding 45825 coupled nonlinear equations which have to be solved numerically.

The LSUBn approximation becomes exact for $n \to \infty$, and so we can improve our results by extrapolating the "raw" LSUBn data to $n \to \infty$. There is ample experience regarding how one should extrapolate the GS energy $e_0(n)$ and the magnetic order parameter $m_s(n)$. For the GS energy per spin $e_0(n) = a_0 + a_1(1/n)^2 + a_2(1/n)^4$ is a reasonable well-tested extrapolation ansatz.[14–17,52–55] An appropriate extrapolation rule for the magnetic order parameter is $m_s(n) = b_0 + b_1(1/n)^{1/2} + b_2(1/n)^{3/2}$.[15–17] Moreover, we know from Refs. 15–17 that the lowest level of approximation called the LSUB2 approximation conforms poorly to these rules. Hence, as in previous calculations,[15–17] we exclude LSUB2 data from the extrapolations.

Note that starting from large J_2 the solution of the CCM-LSUB10 equations can be traced until $J_2 = 0.402$, only. For $J_2 < 0.402$ no CCM-LSUB10 solutions with respect to the collinear stripe reference state could be found. This could be related to the complexity of the set of 45825 coupled equations and the fact that the fully polarized FM state is a low-lying excitation very close to the true GS for $J_2 \sim 0.4$. However, we cannot exclude the possibility that this problem might also be an indication that the collinear stripe order is not a good description for the true GS for J_2 values very close to the transition to the FM GS.

In Fig. 5 we show the GS energy per site for the LSUB6 and LSUB10 approximations, as well as the extrapolated GS energy ($n \to \infty$). The numerical CCM-LSUBn data demonstrate, that the difference between the various LSUBn data is very small (see Fig. 5). As a result, the extrapolated GS energy almost coincides with LSUB10 data (in fact, the difference is less than 0.4%). Moreover, the difference between the extrapolated CCM energy and the finite-size extrapolated ED energy is less than 1% in the whole parameter region. Hence, we conclude that the GS energy data presented in this paper for the FM J_1-J_2 model are very accurate. We again

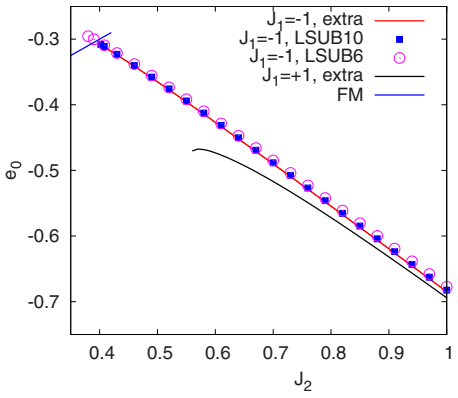

FIG. 5. (Color online) The GS energy per spin as function of J_2 obtained by CCM-LSUBn with $n = 4, 6, 8, 10$ and extrapolated values in the limit $n \to \infty$ using the extrapolation scheme $e(n) = a_0 + a_1(1/n)^2 + a_2(1/n)^4$. For the sake of comparison we show also the extrapolated GS energy for the AFM model (Ref. 17) The blue line shows the energy of the FM eigenstate.

use the intersection point of the energies in order to find an estimate for the transition point J_2^{c1} to the FM GS. We find that $J_2^{c1} = 0.395$ for the LSUB6 approximation and this is shown in Fig. 5. We find also that $J_2^{c1} = 0.394$ and $J_2^{c1} = 0.398$ for the LSUB8 and LSUB4 approximations, respectively (not shown in Fig. 5). As the difference between the LUSB6 and LSUB8 results for J_2^{c1} is already very small we may choose the LSUB8 value, $J_2^{c1} = 0.394$, as the CCM estimate for the transition point. This CCM critical value is in excellent agreement with the ED estimate $J_2^{c1} = 0.393$ (see above). We also compare the GS energies for the FM and the AFM models in Fig. 5. As for the ED method, the deviation in energies between the two models (i.e., negative and positive J_1) becomes substantial at around $J_2 = 0.6$.

We also present the CCM results for spin-spin correlation functions for the FM as well as the AFM model in Fig. 6, where we have shown the same correlation functions as in Fig. 3. Recall that one of the two degenerate collinear stripe states has to be chosen as CCM reference state. As a result the NN correlation functions $\langle \mathbf{s}_0 \cdot \mathbf{s}_\mathbf{R} \rangle$, $\mathbf{R} = (1,0)$, and $\langle \mathbf{s}_0 \cdot \mathbf{s}_\mathbf{R} \rangle$, $\mathbf{R} = (0,1)$, are different, whereas, e.g., all NNN correlation

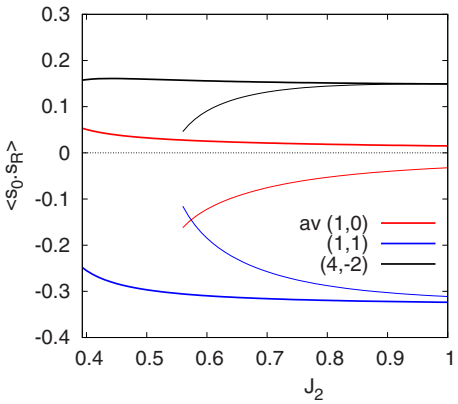

FIG. 6. (Color online) Selected spin-spin correlation functions $\langle \mathbf{s}_0 \cdot \mathbf{s}_\mathbf{R} \rangle$ calculated with CCM within LSUB6 approximation (thick lines: $J_1 = -1$, thin lines $J_1 = +1$).

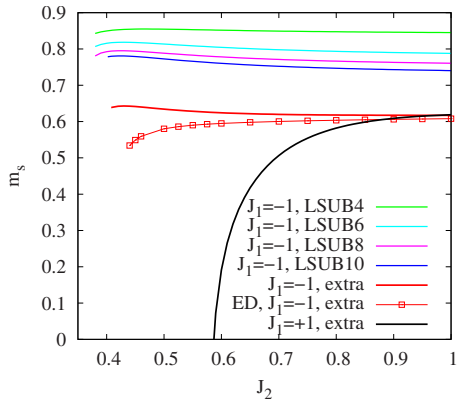

FIG. 7. (Color online) Magnetic order parameter m_s versus J_2 obtained by CCM-LSUBn with $n=4,6,8,10$ and its extrapolated values $(n\to\infty)$ using the extrapolation scheme $m_s(n)=b_0+b_1(1/n)^{1/2}+b_2(1/n)^{3/2}$. By way of comparison we show also the extrapolated collinear stripe order parameter $(n\to\infty)$ for the AFM model $(J_1=+1)$ as well as the extrapolated ED order parameter from Fig. 4.

functions are the same. Hence, we show in Fig. 6 the averaged NN correlation function. For the FM model the agreement of the CCM correlation functions with the ED data is excellent, see Figs. 3 and 6. For the AFM model there is a noticeable difference for $J_2<0.59$. In particular, the steep decrease in the correlation functions at $J_2=0.59$ present in the ED data for the AFM model, cf. Ref. 20, is not observed in the CCM LSUB6 data. For $J_2<0.59$ most likely no magnetic LRO exists for the AFM model.[17] Therefore, it is not surprising that the CCM solution in a finite order of LSUBn approximation based on the collinear stripe reference state does not provide quantitatively precise results for the correlation functions inside the magnetically disordered phase.

Last but not least, we present results for the collinear stripe order parameter m_s calculated by the CCM via Eq. (6) in Fig. 7. For the order parameter, the CCM-LSUBn results depend on the approximation level n more strongly than for the GS energy. Hence, it is more important to extrapolate them in the limit $n\to\infty$. By comparing the correlation functions and the order parameter of the FM model with the AFM model, it is again obvious that both models behave similarly for larger J_2. However, there are significant differences for $J_2\lesssim 0.6$ between both models. Although the CCM result for the AFM model clearly shows the breakdown of the semiclassical collinear magnetic LRO around $J_2=0.6$ [the CCM estimate for the critical frustration is $J_2^{c2}\approx 0.59$ (Ref. 17)], the spin-spin correlation functions and the order parameter for the FM model stay almost constant over the whole parameter region shown in Fig. 7. Again, we obtain good agreement of the order parameter between the ED data and the CCM data in a wide parameter range, cf. Figs. 4 and 7. Only, for $J_2<0.5$ the ED and the CCM order parameters start to deviate slightly from each other, but both parameters stay above 50% of the classical value. Finally, we come to a similar conclusion as in Sec. II that we do not find an indication for the breakdown of the collinear stripe magnetic LRO until $J_2\sim 0.4$ for the FM model.

IV. SUMMARY

In this paper, we have presented results on the GS magnetic ordering of the J_1-J_2 spin-$\frac{1}{2}$ Heisenberg magnet with FM NN exchange $J_1=-1$ on the square lattice obtained by Lanczos ED as well as the CCM. In agreement with previous studies[32–34,37,40,41] we obtain values for the transition point J_2^{c1} at which the fully polarized FM GS (present for small J_2) breaks down, $J_2^{c1}=0.393|J_1|$ (ED) and $J_2^{c1}=0.394|J_1|$ (CCM).

In contrast to previous studies[33,34] we do not find indications for the breakdown of the semiclassical collinear magnetic LRO (present for large J_2) at about $J_2=0.6|J_1|$, rather this magnetic LRO seems to be stable till $J_2\sim 0.4|J_1|$. The question arises why we come to different conclusions than the authors of Refs. 33 and 34. While the conclusions on the breakdown of magnetic long-range order in a quite wide parameter range of the J_1-J_2 model reported in Refs. 33 and 34 is based on ED calculations of the low-energy spectrum of the model for finite lattices up to $N=36$, our reasoning is based on the calculation of spin-spin correlation functions $\langle \mathbf{s}_0\cdot\mathbf{s}_\mathbf{R}\rangle$ and the magnetic order parameter m_s in the GS using ED and CCM. It seems to be natural to consider $\langle \mathbf{s}_0\cdot\mathbf{s}_\mathbf{R}\rangle$ and m_s in order to discuss the existence of GS long-range magnetic order. However, having in mind the numerous studies of the J_1-J_2 model with AFM J_1 over more than 20 years, cf. Refs. 1–21 it is not surprising that a definitive conclusion on the parameter range where magnetic long-range order exists in the model with FM J_1 needs additional investigations by alternative methods.

Although our results are in favor of semiclassical magnetic GS long-range order for a wide range of frustrating exchange J_2, the low-lying excitations and, as a consequence, the low-temperature thermodynamics might be strongly influenced by frustration. This becomes increasingly important when approaching the transition to the FM GS at $J_2^{c1}\approx 0.4|J_1|$, see e.g., Ref. 40. For $J_2\gtrsim J_2^{c1}$ the FM multiplet becomes a low-lying excitation, and so an additional low-energy scale will appear leading, e.g., to an extra low-temperature peak in the specific heat, see, e.g., Refs. 32, 56, and 57.

Stimulated by the recent experimental activities and the related search for new square-lattice materials near the quantum critical point of the J_1-J_2 model, the issue of low-lying excitations and their relevance for the thermodynamic properties should be investigated in future studies in more detail.

ACKNOWLEDGMENT

We thank S. E. Krüger and R. Zinke for valuable discussions. This work was supported by the DFG (Grant No. Ri615/16-1). J.R. thanks the Max-Planck-Institut für Physik komplexer Systeme for the hospitality during his visit in the Advanced Study Group "Unconventional Magnetism in High Fields" in April 2010 and the members of the Group for valuable discussions.

[1] P. Chandra and B. Doucot, Phys. Rev. B **38**, 9335 (1988).
[2] E. Dagotto and A. Moreo, Phys. Rev. Lett. **63**, 2148 (1989).
[3] F. Figueirido, A. Karlhede, S. Kivelson, S. Sondhi, M. Rocek, and D. S. Rokhsar, Phys. Rev. B **41**, 4619 (1990).
[4] H. J. Schulz and T. A. L. Ziman, EPL **18**, 355 (1992); H. J. Schulz, T. A. L. Ziman, and D. Poilblanc, J. Phys. I **6**, 675 (1996).
[5] J. Richter, Phys. Rev. B **47**, 5794 (1993).
[6] J. Richter, N. B. Ivanov, and K. Retzlaff, EPL **25**, 545 (1994).
[7] M. E. Zhitomirsky and K. Ueda, Phys. Rev. B **54**, 9007 (1996).
[8] A. E. Trumper, L. O. Manuel, C. J. Gazza, and H. A. Ceccatto, Phys. Rev. Lett. **78**, 2216 (1997).
[9] R. F. Bishop, D. J. J. Farnell, and J. B. Parkinson, Phys. Rev. B **58**, 6394 (1998).
[10] L. Capriotti, F. Becca, A. Parola, and S. Sorella, Phys. Rev. Lett. **87**, 097201 (2001).
[11] L. Siurakshina, D. Ihle, and R. Hayn, Phys. Rev. B **64**, 104406 (2001).
[12] R. R. P. Singh, Weihong Zheng, J. Oitmaa, O. P. Sushkov, and C. J. Hamer, Phys. Rev. Lett. **91**, 017201 (2003).
[13] J. Sirker, Z. Weihong, O. P. Sushkov, and J. Oitmaa, Phys. Rev. B **73**, 184420 (2006).
[14] D. Schmalfuß, R. Darradi, J. Richter, J. Schulenburg, and D. Ihle, Phys. Rev. Lett. **97**, 157201 (2006).
[15] R. F. Bishop, P. H. Y. Li, R. Darradi, and J. Richter, J. Phys.: Condens. Matter **20**, 255251 (2008).
[16] R. F. Bishop, P. H. Y. Li, R. Darradi, J. Schulenburg, and J. Richter, Phys. Rev. B **78**, 054412 (2008).
[17] R. Darradi, O. Derzhko, R. Zinke, J. Schulenburg, S. E. Krüger, and J. Richter, Phys. Rev. B **78**, 214415 (2008).
[18] T. Pardini and R. R. P. Singh, Phys. Rev. B **79**, 094413 (2009).
[19] V. Murg, F. Verstraete, and J. I. Cirac, Phys. Rev. B **79**, 195119 (2009).
[20] J. Richter and J. Schulenburg, Eur. Phys. J. B **73**, 117 (2010).
[21] J. Reuther and P. Wölfle, Phys. Rev. B **81**, 144410 (2010).
[22] E. E. Kaul, H. Rosner, N. Shannon, R. V. Shpanchenko, and C. Geibel, J. Magn. Magn. Mater. **272-276**, 922 (2004).
[23] M. Skoulatos, J. P. Goff, N. Shannon, E. E. Kaul, C. Geibel, A. P. Murani, M. Enderle, and A. R. Wildes, J. Magn. Magn. Mater. **310**, 1257 (2007).
[24] P. Carretta, M. Filibian, R. Nath, C. Geibel, and P. J. C. King, Phys. Rev. B **79**, 224432 (2009).
[25] M. Skoulatos, J. P. Goff, C. Geibel, E. E. Kaul, R. Nath, N. Shannon, B. Schmidt, A. P. Murani, P. P. Deen, M. Enderle, and A. R. Wildes, EPL **88**, 57005 (2009).
[26] R. Nath, Y. Furukawa, F. Borsa, E. E. Kaul, M. Baenitz, C. Geibel, and D. C. Johnston, Phys. Rev. B **80**, 214430 (2009).
[27] H. Kageyama, T. Kitano, N. Oba, M. Nishi, S. Nagai, K. Hirota, L. Viciu, J. B. Wiley, J. Yasuda, Y. Baba, Y. Ajiro, and K. Yoshimura, J. Phys. Soc. Jpn. **74**, 1702 (2005).
[28] A. A. Tsirlin and H. Rosner, Phys. Rev. B **79**, 214417 (2009).
[29] A. A. Tsirlin, B. Schmidt, Y. Skourski, R. Nath, C. Geibel, and H. Rosner, Phys. Rev. B **80**, 132407 (2009).
[30] R. Nath, A. A. Tsirlin, H. Rosner, and C. Geibel, Phys. Rev. B **78**, 064422 (2008).
[31] A. A. Tsirlin, R. Nath, A. M. Abakumov, R. V. Shpanchenko, C. Geibel, and H. Rosner, arXiv:0910.2258, Phys. Rev. B (to be published).
[32] N. Shannon, B. Schmidt, K. Penc, and P. Thalmeier, Eur. Phys. J. B **38**, 599 (2004).
[33] N. Shannon, T. Momoi, and P. Sindzingre, Phys. Rev. Lett. **96**, 027213 (2006).
[34] P. Sindzingre, N. Shannon, and T. Momoi, J. Magn. Magn. Mater. **310**, 1340 (2007).
[35] B. Schmidt, N. Shannon, and P. Thalmeier, J. Phys.: Condens. Matter **19**, 145211 (2007).
[36] B. Schmidt, N. Shannon, and P. Thalmeier, J. Magn. Magn. Mater. **310**, 1231 (2007).
[37] J. R. Viana and J. R. de Sousa, Phys. Rev. B **75**, 052403 (2007).
[38] P. Sindzingre, L. Seabra, N. Shannon, and T. Momoi, J. Phys.: Conf. Ser. **145**, 012048 (2009).
[39] P. Sindzingre, N. Shannon, and T. Momoi, arXiv:0907.4163 (unpublished).
[40] M. Härtel, J. Richter, D. Ihle, and S.-L. Drechsler, Phys. Rev. B **81**, 174421 (2010).
[41] D. V. Dmitriev, V. Ya. Krivnov, and A. A. Ovchinnikov, Phys. Rev. B **55**, 3620 (1997).
[42] T. Munehisa and Y. Munehisa, J. Phys.: Condens. Matter **19**, 196202 (2007).
[43] T. Kashima and M. Imada, J. Phys. Soc. Jpn. **70**, 3052 (2001).
[44] J. Richter, J. Schulenburg, and A. Honecker, in *Quantum Magnetism*, edited by U. Schollwöck, J. Richter, D. J. J. Farnell, and R. F. Bishop, Lecture Notes in Physics Vol. 645, (Springer, Berlin, 2004), p. 85.
[45] A. Läuchli, J. C. Domenge, C. Lhuillier, P. Sindzingre, and M. Troyer, Phys. Rev. Lett. **95**, 137206 (2005).
[46] J. Richter, J. Schulenburg, A. Honecker, and D. Schmalfuß, Phys. Rev. B **70**, 174454 (2004).
[47] J. Schulenburg, A. Honecker, J. Schnack, J. Richter, and H.-J. Schmidt, Phys. Rev. Lett. **88**, 167207 (2002); A. Honecker, J. Schulenburg, and J. Richter, J. Phys.: Condens. Matter **16**, S749 (2004).
[48] The spin-spin correlation functions for $N=20$, 32, and 36 can be provided upon request.
[49] H. Neuberger and T. Ziman, Phys. Rev. B **39**, 2608 (1989).
[50] P. Hasenfratz and F. Niedermayer, Z. Phys. B: Condens. Matter **92**, 91 (1993).
[51] C. Zeng, D. J. J. Farnell, and R. F. Bishop, J. Stat. Phys. **90**, 327 (1998).
[52] R. F. Bishop, D. J. J. Farnell, S. E. Krüger, J. B. Parkinson, J. Richter, and C. Zeng, J. Phys.: Condens. Matter **12**, 6887 (2000).
[53] D. J. J. Farnell and R. F. Bishop, in *Quantum Magnetism, Lecture Notes in Physics*, edited by U. Schollwöck, J. Richter, D. J. J. Farnell, and R. F. Bishop (Springer, Berlin, 2004), Vol. 645, p. 307.
[54] S. E. Krüger, J. Richter, J. Schulenburg, D. J. J. Farnell, and R. F. Bishop, Phys. Rev. B **61**, 14607 (2000).
[55] R. Darradi, J. Richter, and D. J. J. Farnell, Phys. Rev. B **72**, 104425 (2005).
[56] F. Heidrich-Meisner, A. Honecker, and T. Vekua, Phys. Rev. B **74**, 020403(R) (2006).
[57] H. T. Lu and Y. J. Wang, Shaojin Qin, and T. Xiang, Phys. Rev. B **74**, 134425 (2006).